Mechanics of Polymer−Clay Nanocomposites

YuanQiao Rao* and John M. Pochan

Research Laboratories, Eastman Kodak Company, 1999 Lake Avenue, Rochester, New York 14650-2158

Received June 27, 2006; Revised Manuscript Received October 9, 2006

ABSTRACT: The mechanics of nanocomposites is critical in the design of nanomaterials with desirable properties. In this paper, the mechanics of polymer−clay nanocomposites is studied using a designed polymer and solution nanocomposite synthesis. A copolymer latex, with function groups that strongly interact with the surface of the clay nanoplatelet and glass-transition temperature lower than room temperature, was synthesized. Uniformly dispersed nanocomposites were then generated using water as the intercalation agent through the solution process. The chain mobility in the nanocomposites is greatly reduced as studied by dynamic mechanical thermal analysis (DMTA) and dielectric thermal analysis (DETA). The modulus of the composite increases significantly. The modulus enhancement strongly relates to the volume of the added clay as well as the volume of the constrained polymer. This modulus enhancement follows a power law with the content of the clay and is modeled well by Mooney's equation for this soft-polymer-based nanocomposite. Modeling suggests that the nanocomposite modulus enhancement is determined by the high aspect ratio of the intercalated clay and the strong interfacial strength, in the form of the Einstein coefficient, K, when the modulus of the matrix phase is much lower than that of the clay, i.e., $E_f/E_m > 100$. This study also indicates that the structure of clay nanocomposites with strong interfacial interactions is analogous to that of semicrystalline polymers. In the case of polymer−clay nanocomposites, the intercalated clay phase serves as an unmeltable crystalline phase that results in improvement in mechanical and thermal properties.

Introduction

Nanocomposites generate a great deal of interest from materials scientists because of their potentially novel properties. Pioneering work at Toyota has stimulated research on polymer−clay nanocomposites.[1−3] It has been shown that a combined enhancement of modulus, strength, and toughness was achieved in an exfoliated Nylon 6−clay nanocomposite. However, the property enhancement depends very much on the chosen nanocomposite system. Many nanocomposite systems do not give the same degree of property enhancement, as does a polyamide−clay nanocomposite.[1−4] There has been a long-standing debate on how important the clay exfoliation is in affecting the properties. The lower degree in property enhancement has often been attributed to the difficulty to achieve clay exfoliation.

The clay used in nanocomposites is usually a type of smectite clay. Chemically, it is a metal silicate. It tends to form small crystallites of a lamellar structure comprising repeated sheets of two silica tetrahedral layers with an edge-shared octahedral metal oxide layer. There is net negative charge in the clay single sheet because of the valance imbalance in the structure. The net negative charge is then balanced by the more mobile positive charge on the face. Clay crystals have a constant interlayer distance that is determined by the type of counter ions present. Smaller ions such as Na^+, K^+, or Li^+ in pristine clay lead to a smaller interlayer distance and thus a tightly spaced clay stack. The interlayer distance of the pristine clay is typically about 10 Å. When this type of clay is added to thermoplastic polymers, shear force is used to break the stacking of the clay. If the stacking order is completely lost, the clay is identified as exfoliated or in an exfoliation state. However, the strong electrostatic force often makes the clay gallery difficult to exfoliate. Organic modification is then used to expand the interlayer spacing so as to improve the possibility of the polymer chain entering the clay interlayer space.[5] When a larger size organic cationic group replaces the metal counterion to make the clay more organophilic, the interlayer spacing is usually larger than that of the pristine inorganic clay. The clay is now identified as intercalated or in an intercalation state. The state of the clay in nanocomposites can be studied by X-ray diffraction (XRD). The complete disappearance of the (001) peak indicates the state of exfoliation. The shift of (001) peak to a lower 2θ indicates the state of intercalation. A previous study showed that the clay in the matrix often has a distribution of states: partially exfoliated, partially intercalated, and partially pristine. These states have made it difficult to systematically understand the mechanics of nanocomposites.[6]

Not only should the dispersion of the clay nanoparticles in a polymer nanocomposite be addressed, but also the interfacial phase in nanocomposites needs to be considered because of the large surface area presented by the nanosized fillers. Different instruments have been used to study the interfacial interaction in the polymer−clay nanocomposites: thermally stimulated current (TSC),[7] modulated temperature differential scanning calorimetry (MTDSC),[8] dynamic mechanical thermal analysis (DMTA),[9] photoacoustic Fourier transform infrared spectroscopy (PA FTIR),[10] and terahertz spectroscopy (THz).[11] Although ionic interactions,[11] H-bonding,[10] and nonbonding interactions[10] were observed, there has been limited research on how these interactions affect the mechanical properties of the nanocomposites and how polymers can be properly designed to have a controlled interaction with the clay nanoplatelets.

Different composite theories were used to correlate the modulus with the volume fraction of the nanoclay filler and the aspect ratio of the clay.[6,12,13] An effective particle was proposed to better represent the nanofiller.[6] The Halpin−Tsai equation with modification has been shown to predict reasonable the composite modulus. Most studies assumed that the high

* Corresponding author. E-mail: yuanqiao.rao@kodak.com.

10.1021/ma061445w CCC: $37.00
Published on Web 12/16/2006

aspect ratio of the nanoparticles is important. This has been validated by several studies where clay particles of different aspect ratios were used in the formation of the nanocomposites.[13,14] Meanwhile, work on other nanofiller systems indicate significant property enhancement can be achieved using other types of low aspect ratio nanofiller where the matrix filler interaction may be more important.[15]

It is this paper's objective to provide some insight into the micromechanics of polymer−clay nanocomposites. A polymer was designed and synthesized with function groups that strongly interact with the surface of the clay nanoplatelets. The complication of the nonuniform particle dispersion was addressed using a solution process, and a uniformly intercalated and dispersed polymer clay nanocomposite was generated. The reduction in the chain mobility was studied, and the mechanics of the composites was probed.

Experimental

A copolymer latex ($PBSMaSO_3$) was synthesized through emulsion polymerization. $PBSMaSO_3$ is composed of butyl acrylate (59 mol %), styrene (25 mol %), methacrylamide (8 mol %), and 2-acrylamido-2-methylpropane sulfonic acid, sodium salt (8 mol %). The glass-transition temperature (T_g) of the dried film of $PBSMaSO_3$ is 20 °C. Montmorillonite clay (Cloisite Na^+) was supplied by Southern Clay Products and used as is, with a reported aspect ratio (length/thickness, L/t) of 200. A 3 wt % aqueous Cloisite Na^+ dispersion was made by vigorous mixing and centrifuging to remove any impurities. The resulting dispersion remained in colloidal dispersion without settlement for months. $PBSMaSO_3$ latex was then added to the clay dispersion at different ratios of polymer to clay, and the sol was mixed well. The resultant solution was poured into a 10 cm × 10 cm Teflon cast overlaid by Kapton film. The solution was dried at ambient condition in the cast. The cast film was peeled from the cast and further dried in a vacuum oven for 2 days at room temperature before further testing.

The structure of the nanocomposite, in particular, the state of intercalation of the clay, was investigated by XRD. For XRD analysis, a Rigaku RU-300 Bragg−Brentano diffractometer with a scintillation point detector was used. The film was deposited on a substrate. XRD was done in reflection mode to explore mainly the (001) of the polymer−clay nanocomposites. The mechanical properties of the films were measured using a Sintech mechanical tester. At least three samples were run, and the average is presented. The chain constraint and the thermal behavior of the material were studied with a DMTA (Rheometrics Scientific RSAII) and dielectric thermal analyzer (DETA) (Novocontrol). The DMTA was run at 2 °C/min and 10 Hz, and the DETA was run at 25 °C.

Results and Discussion

Chain Constraint in Polymer−Clay Nanocomposites. The challenge in polymer−clay nanocomposites has been to have a uniformly dispersed nanofiller phase in the matrix and a filler phase size less than several hundreds of nanometers. It has often been reported that there are different domains of the clay filler either in an exfoliated state, an intercalated state, or in the pristine state.[16] The mixture of the clay states is attributed to the tendency of the self-organization of the clay and the agglomeration caused by the large surface area of the nanoparticles. The clay used in this study is a montmorillonite clay and has a chemical structure of $Na^{c+}[(Si_xAl_yMg_z)O_a(OH)_b]^{c-}$. The occupation by an Mg atom instead of Al in some locations generates a net negative charge on each sheet. The c-axis of the stacked clay gallery is formed through weak dipolar and van der Waals interaction.

It is possible to break the gallery by breaking the ionic interaction using water. Water has been shown to be an effective intercalation agent.[17] By using an aqueous blending process, a water-soluble polymer or water-dispersible polymer can be introduced to the surface of the individual clay nanoplatelet so as to form a new clay nanophase. This new clay nanophase can be either exfoliated, where the clay nanophase comprises only one clay nanosheet, or intercalated, where the clay nanophase comprises several layers of alternating clay nanosheets and the embedded polymer layers with (00l) at a lower 2θ. There has been limited research on this nanocomposite synthesis method;[18−21] in particular, there has been no reported work with soft latex and clay.

In our study, a latex polymer comprising butyl acrylate, styrene, methacrylamide, and 2-acrylamido-2-methylpropane sulfonic acid sodium salt was designed to control its interaction with clay. In this polymer, butyl acrylate and styrene mainly adjust the T_g of the material; methacrylamide is designed to form hydrogen bonds with the surface oxygen of the clay platelet and an anionic sulfonic salt is used to separate the polymer from the surface to extend the intercalation spacing. The anionic charge on the polymer further stabilizes and prevents the agglomeration of the formed nanophases. The presence of methacrylamide and 2-acrylamido-2-methylpropane sulfonic acid sodium salt makes the latex self-dispersive in water with a hydrophilic surface.

Good films were formed after casting the mixture because of the low T_g of the latex. This low T_g latex also allows for the investigation of the polymer−clay nanocomposites at a temperature higher than the T_g of the polymer. The use of water and the latex makes good clay intercalation and uniform dispersion of the nanofillers in the matrix. On the other hand, it is difficult to generate well-dispersed intercalated nanocomposites via melt processing. The temperature used in most melt processing does not disrupt the ionic interaction that interferes with clay intercalation. Thus, the clay platelet usually needs to be pretreated with organic surfactants, typically quaternary amine.[2] This small molecule tends to degrade at the temperature of processing so as to cause the degradation of the formed nanocomposites.

The generated film samples range from transparent when clay loading is less than 10 wt % to uniformly translucent between 10 and 17 wt % of clay loading. This suggests that the nanophase in the composite is less than 200 nm and nanocomposites are obtained in the investigated range of clay loading. The dispersion quality of the $PBSMaSO_3$−clay nanocomposite was investigated by XRD. As shown in Figure 1a, the nanocomposite is exfoliated when the clay loading is less than 4 wt %, and the nanocomposite was intercalated when the clay loading is higher. The (001) peak of the nanocomposite with 25 wt % clay in Figure 1a and b is a nice symmetric peak when the baseline is corrected and an additional higher order of (00l) peaks is shown. This indicates the uniformity of the dispersion and the well-ordered intercalated phase formed through the solution processing. The thickness of the new nanophase is calculated to be 40 Å using Scherrer's technique based on Figure 1b.

It is of interest to learn about the mobility of the polymers inside the clay gallery. We also want to learn how the presence of the clay galleries affects the mobility of the surrounding polymers. DMTA and DETA were used to study the chain mobility. During the glass transition, the long-range polymer chain gains mobility and thus dissipates a great amount of energy through viscous movement. This is shown in the tan δ peak in a DMTA test. Therefore, any depression in tan δ indicates the reduction of the number of the mobile chains during the glass transition. The relative peak height or area is proportional to

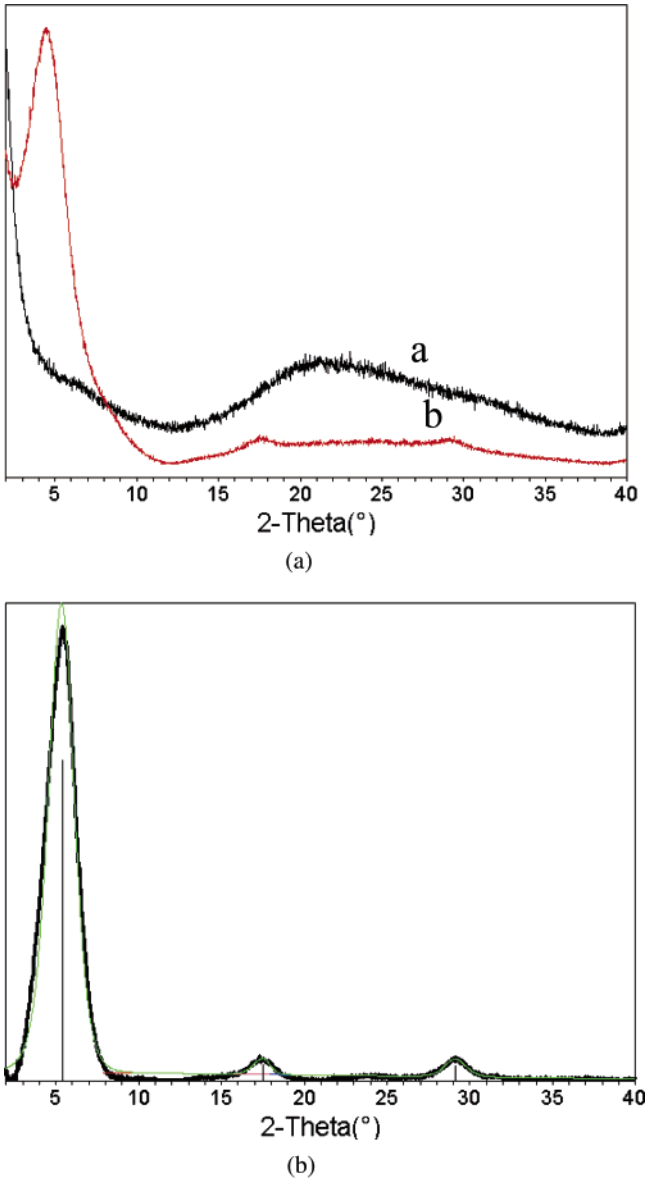

Figure 1. X-ray diffraction pattern of two exemplary $PBSMaSO_3$−clay nanocomposites: (a) XRD patterns: a. $PBSMaSO_3$−clay = 96:4 (wt %); b. $PBSMaSO_3$−clay = 75:25 (wt %); (b) XRD pattern of sample $PBSMaSO_3$−clay = 75:25 (wt %) after baseline correction. The black line is the scan trace and the green line is the peak fitting result.

the volume of the constrained chains.[23] Similarly, by measuring the induced polarization, DETA can quantify the amount of material participating in the glass transition. The height of the imaginary part of the dielectric constant (ϵ'') is proportional to the number of the mobile dipoles during the glass transition.[22] Thus, the decrease in the ϵ'' characterizes the immobilization of the polymer chains. This quantitative measurement of constraint chains was first developed to study the crystallinity of semicrystalline polymers.[23] Recently, the measurement was also used to calculate the constrained polymer volume in a polymer−clay nanocomposite.[9,24,25] Both DMTA and DETA studies suggest that a significant portion of polymer chains become immobilized in the clay nanocomposites (Figure 2). However, two measurements provide some different information. The DMTA scan indicates that the glass transition of the remaining mobile chains shifts to a lower temperature with the addition of clay nanoplatelets, while the DETA scan shows that the glass transition of the remaining mobile chains remains the

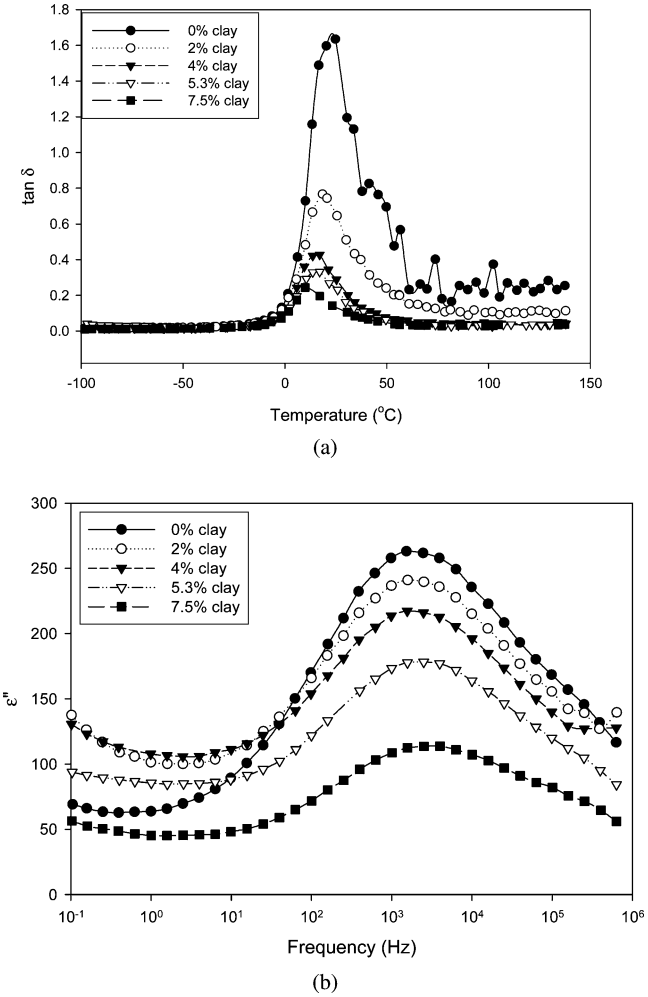

Figure 2. Chain constraint in polymer clay nanocomposites studied by DMTA and DETA: (a) trace of tan δ vs temperature as measured by DMTA at 10 Hz, (b) trace of ϵ'' vs frequency as measured by DETA at room temperature (the percentage in legends are volume percentage).

same. The amount of constrained chains is also different as calculated from DMTA and DETA. DMTA shows that the volume of the constrained chains is as high as 87% with a 7 vol % addition of the clay nanofiller, assuming that the density of the clay is 2.6 g/cm^3 and the density of the polymer is 1 g/cm^3 (Figure 2a). In comparison, DETA gives a lower amount of constrained chain percentage of 60%. The difference in the two measurements is speculated to be caused by the compositional inhomogeneity in the copolymer. Because DETA is detecting a dipole moment and DMTA is detecting mechanical deformation, different chain segment sensitivities may thus cause differences in measurement.

The constrained chain volume changes with the amount of clay filler in a power law relation. As shown in Figure 3, the data follow very well with the fitted curve. According to DMTA,

$$\ln V_{con} = 0.36 \ln V + 3.7 \quad (1)$$

and according to DETA,

$$\ln V_{con} = 1.71 \ln V + 0.6 \quad (2)$$

where V_{con} is the percentage of constrained polymer chains and V is the volume percentage of the added clay.

It was noted earlier that a small amount of clay immobilizes a significant amount of polymer chain during the glass transition. It is important to understand how this affects the structure and

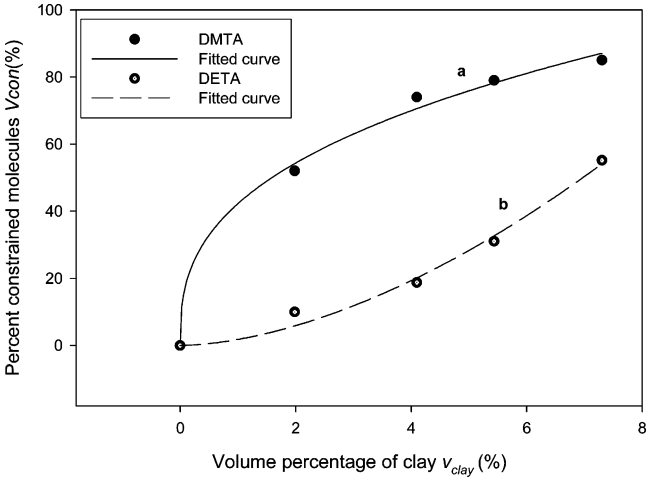

Figure 3. Percentage of the constrained chain calculated using tan δ peak value in DMTA (solid dot) and ϵ'' in DETA (open dot) vs added clay volume in nanocomposites and the fitted curves.

Table 1. Basal Spacing of Intercalated Clay vs Clay Amount in PBSMaSO$_3$−Clay Nanocomposites

amount of clay (wt %)	basal plane spacing (Å)
4	exfoliated
5	37.7
8	29.8
10	27.6
12	24.8
13	26.5
17	22.6
17	24.8
25	19.3
40	16.2
Pure clay	12.9

Table 2. Modulus of the Clay−PSBMaSO$_3$ Nanocomposite Film

clay amount		Young's modulus (MPa)	
wt %	vol %	at RT	at 100 °C
0	0	35	0.6
5	2	88	39
10	4	190	190
13	5.4	402	405
17	7.3	798	1170

the mechanical properties of the nanocomposites. X-ray diffraction was used to further study the structure of the nanocomposites. The change in (001) spacing with different amounts of clay is summarized in Table 1. It is noted that the (001) spacing of the intercalated clay decreases with the increasing amount of clay. It is speculated that this is attributed to a partition equilibrium process. During the drying following the casting, polymer chains develop an interaction with clay sheets, and clay sheets also self-organize. There is association equilibrium between polymer and clay during the process, and a polymer can form bonds with another polymer or a clay. In the beginning of the process, one layer of polymer is absorbed onto the face of the clay sheet. When there is more clay, the absorbed polymer is more likely to associate with another clay surface or another absorbed polymer rather than with another free polymer, and thus the distance between two clay sheets is smaller, leading to a smaller basal spacing at a higher level of clay loading.

The reduced mobility and the increased modulus at higher temperature, as seen in Table 2 when measured by DMTA, imply the crosslinking characteristic[27,28] of the polymer−clay nanocomposites. A structural model is proposed, as shown in Figure 4. In this model, the clay nanofillers are first intercalated; new nanophase (B in Figure 4) are formed from the intercalated clay. Further, these nanoparticles reduce the mobility of the surrounding polymers. There is an effective constraint length, and polymers lose their mobility during glass transition when the polymer chain is within this constraint length (C in Figure 4). The intercalated nanophase (B in Figure 4) and the constrained phase (C in Figure 4) form an effective particle with an effective volume much higher than that of the clay. Structurally, the nanocomposite is analogous to a semicrystalline polymer, where the intercalated clay is similar to the crystalline domain.

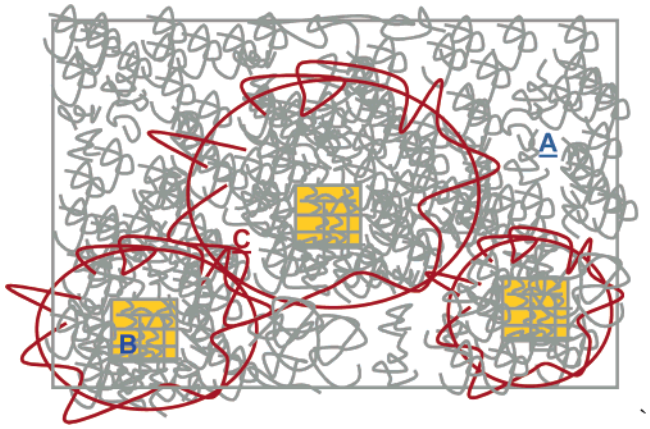

Figure 4. Schematic of the proposed morphology of PBSMaSO$_3$−clay nanocomposites.

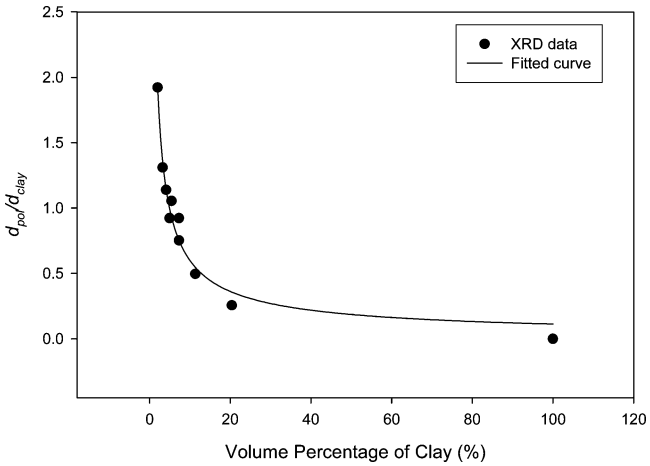

Figure 5. Plot of the d_{pol}/d_{clay} vs the volume fraction of the added clay.

The results of the polymer constraint measurement and the X-ray study are integrated to further illustrate the structure of the nanocomposites, especially the constrained polymer. The embedded polymer chain thickness (d_{pol}) in an intercalated clay is calculated by subtracting the d_{001} (shown in Table 1) in an intercalated clay by the thickness of a clay single crystal (d_{clay}), which is 12.9 Å. There is a clear correlation between d_{pol} and V (the volume fraction of the clay), as shown in Figure 5. According to the data,

$$d_{pol}/d_{clay} = 3.15\ V^{-0.7} \qquad (3)$$

where V is the volume fraction of the clay, and d_{pol} and d_{clay} are the occupied thicknesses of the polymer and clay, respectively, between two clay sheets.

It is assumed that the clay single crystal bonds strongly with segments of the polymer. These polymer segments are embed-

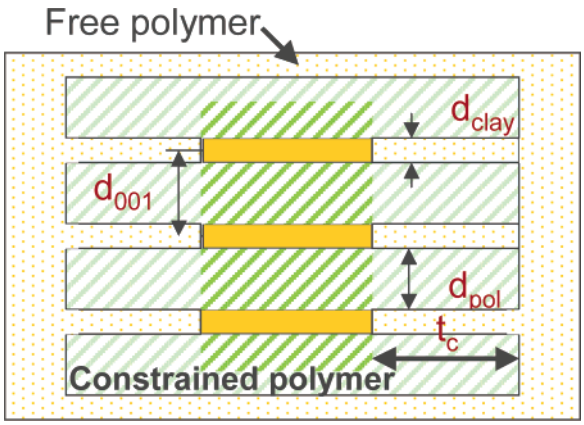

Figure 6. Idealized compositional model of one composite unit in polymer−clay nanocomposites.

ded between sheets of clay. As these polymer segments are parts of polymer chains, the involved polymer chains are also constrained. The effective constrained polymer volume is much higher because of this extended constraint zone. A model structure is proposed, as shown in Figure 6.

Figure 6 is a schematic of an average structural unit in a polymer−clay nanocomposite, where d_{clay} is the thickness of a clay single crystal, d_{pol} is the thickness of embedded polymers, and d_{001} is the thickness of a combined layer of a clay crystal and an embedded polymer layer. There is an average of n layers of clay sheets in one unit. An effective clay particle is then formed of n layers of clay sheets and the embedded polymers. It is assumed that one effective clay particle has an effective constraining length, t_c, and all the polymers within this distance to the clay surface are constrained. In a polymer−clay nanocomposite, assuming the clay volume percentage is V, the polymer volume percentage is V_p, the constrained polymer volume percentage is V_c, and the clay single crystal is a disc with a radius of a, the clay volume in one structural unit is

$$V^*_{clay} = 3.14\, a^2 \cdot d_{clay} \cdot n \tag{4}$$

the volume of the constrained polymers is

$$\begin{aligned} V^*_{pol} &= 3.14(a + t_c)^2 (d_{pol}) \cdot (n + 1) - V^*_{clay} \\ &= 3.14(a + t_c)^2 (d_{pol}) \cdot (n + 1) - 3.14 a^2 \cdot d_{clay} \cdot n \end{aligned} \tag{5}$$

and the number of units in a composite is

$$N = V/V^*_{clay} = \nu/(3.14 a^2 \cdot d_{clay} \cdot n) \tag{6}$$

The volume percentage of constrained polymers to overall polymers is

$$V_{con} = V^*_{pol} \cdot N/(100 - V) \cdot 100 \tag{7}$$

Replacing d_{pol} in eq 6 by eq 3 and when V is small, eq 7 can be further simplified as

$$V_{con} = (1 + 1/n)(1 + t_c/a)^2 V^{0.35} \tag{8}$$

As a scaling law,

$$V_{con} \propto b \cdot V^{0.35} \tag{9}$$

where V_{con} is the percentage of constrained polymer chains, V is the volume percentage of added clay, n is the number of layers in one effective nanoparticle, t_c is the effective constraint length, and a is the radius of the clay single-crystal disc.

The good agreement between eqs 9 and 1 supports our proposed structural model (Figure 6). Fundamentally, it implies that the polymer chain constraint by the nanoparticles depends on the size of the effective constraint zone, t_c. The effect of the degree of intercalation or exfoliation on the chain constraint plays a limited role as represented by n.

Young's Modulus of Polymer−Clay Nanocomposites. In the earlier discussion, a structural model of PBSMaSO_3−clay nanocomposites was developed. It indicates that the interaction between clay and a polymer chain is an important aspect of the structure. This interaction further influences the effective constraint zone or an interfacial zone, which is another way to describe it. With this molecular structural model, the micromechanics of polymer−clay nanocomposites and the effect of the structure on the properties of nanocomposites are studied. Modulus is one of the well-understood mechanical properties. It is used here to probe the mechanics of nanocomposites. The synthesized nanocomposite films have improved mechanical properties: more than a 20 times increase in modulus and a 4 times increase in strength at a 17 wt % loading of clay. The change of Young's modulus with different amounts of clay is summarized in Table 2. This is the highest ratio reported so far of the composite−matrix modulus in clay nanocomposites. There has been some previous research performed on soft material−clay composites, and the composite−matrix modulus ratio was reported then to be under 4.[26] The best thermoplastic material−composite modulus ratio was reported on the nylon 6−clay composite, which is 2.[2]

The effect of molecular weight, crosslinking density, and crystallinity were extensively studied in the micromechanics of polymers.[28,29] It is natural for us to examine the existing models. In general, the effect of crystallinity on the modulus follows the following relation:[29]

$$\log_{10} G = 5.763 + 4.77 V_c \tag{10}$$

where G is the shear modulus in Pa of the semicrystalline polymer, and V_c is the volume fraction of the crystalline phase. In the case of polymer−clay nanocomposites, V_{con} is replacing V_c. Two prefactors can change. Thus, eq 10 can be rewritten as:

$$\log_{10} E = a_1 + a_2 V_{con} \tag{11}$$

where E is the Young's modulus in MPa of the polymer−clay nanocomposite, V_{con} is the volume percentage of the constrained polymer, a_1 is the modulus of the matrix, and a_2 is a constant. The moduli at 100 °C (Table 2) fit well to eq 11, as shown in Figure 7.

The above discussion further supports our speculation of the structure of nanocomposites. In a polymer−clay nanocomposite, the nanoparticles create crosslinking of the matrix by interacting strongly with the polymer chain and limiting the mobility of surrounding chains. The question remains in the understanding of the parameter a_2 in eq11. In general, a_2 can be regarded as a function of the particle property and the interfacial property. Molecular mechanics, in particular Mooney's theory,[30] can then be explored. The original Mooney's treatment studied the effect of spherical fillers on the viscosity of a concentrated colloid fluid. Taking its analogue of modulus for polymer material and expanding the shape into nonspherical ones, it was proposed that when the modulus of the filler is much higher than that of

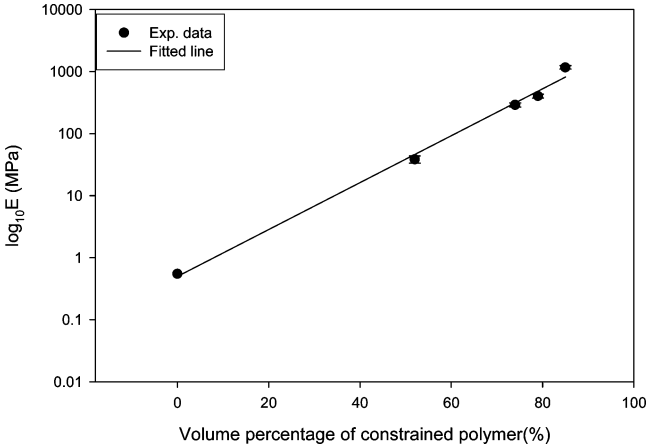

Figure 7. Dependence of the Young's modulus of nanocomposites on the constrained polymer.

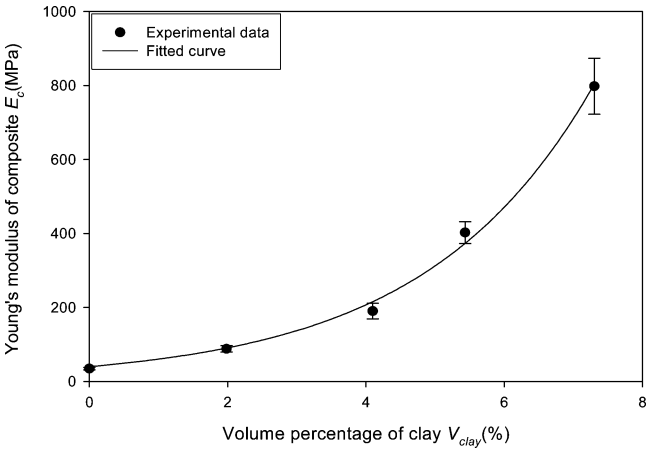

Figure 8. Experimental modulus data and the fitted model.

the matrix, the modulus increase can be described by the modified Mooney equation:

$$\ln \frac{E}{E_1} = \frac{k_E \phi_2}{1 - \phi_2/\phi_m} \tag{12}$$

where E is the modulus of the nanocomposite, E_1 is the modulus of the matrix, K_E is the Einstein coefficient, ϕ_2 is the volume fraction of the filler, and ϕ_m is the maximum volume fraction that the filler can have. K_E is a function of the interaction between the filler and the matrix as well as the aspect ratio of the filler. The stronger the interaction and the higher the aspect ratio of the filler, the higher the K_E is. The strong interaction between the clay and the polymer ensures a nonslippage interface. Under the nonslippage condition:

$$K_E = 2.5 \cdot (L/t)^{0.645} \tag{13}$$

An excellent fit is achieved when this Mooney power function is used to describe the observed modulus change with the amount of added clay, as shown in Figure 8. The regressed K_E is 40. The L/t of the clay domain, which is the effective nanophase, is then calculated to be 74 by using eq 13. It is noted in the previous section that the thickness of the nanophase in the nanocomposites is 40 Å. Thus, the average aspect ratio (L/t) is calculated to be about 50 according to XRD. At the first approximation, the two analyses agree with each other. This aspect ratio indicates that, on average, each intercalated clay domain comprises three layers of clay sheets with the intercalated polymer chain. This also illustrates, in eq 11, how a_2 is related to the interfacial strength and the aspect ratio of the clay particle.

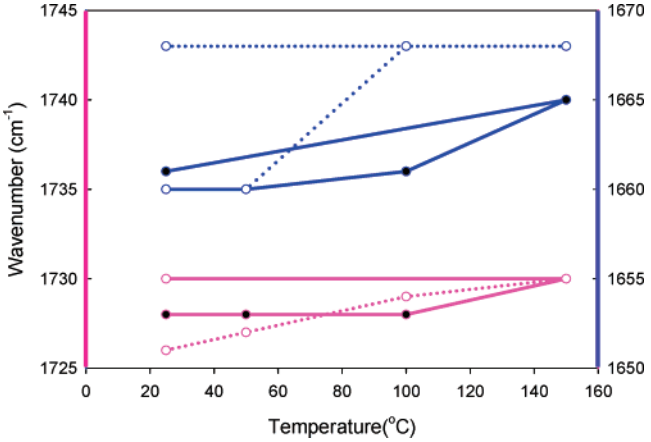

Figure 9. Change of the carbonyl IR absorption peak with temperature for polymer (solid line) and polymer−clay nanocomposite (dotted line).

The study suggests the applicability of Mooney's equation in describing the Young's modulus of polymer−clay nanocomposites when the matrix is in a rubbery state. It is proposed that a new form of K_E can be used to incorporate the strength of the interfacial interaction.

ATR-FTIR was used to examine the origin of the strong interaction between clay and polymer. The samples of polymer and polymer−clay composite (85:15 wt ratio) were first conditioned at 23 °C/50% RH for at least a day. Then an in-situ FTIR measurement was done while the samples were heated to different temperatures: 25, 50, 100, and 150 °C, and then cooled back to room temperature. The peak frequency of the two carbonyls in both samples indicates the existence of H bonding. The shift of carbonyl stretching peak of room-temperature samples, from 1728 cm^{-1} of the latex polymer to a lower wavelength of 1726 cm^{-1} in the latex−clay composite, suggests a stronger hydrogen bond is formed between the polymer and the clay. When the samples are heated, both carbonyl groups move to a higher frequency with increasing temperature. However, the shifts of polymer and polymer−clay composite follow a different pattern, as seen in Figure 9, suggesting that the nature of these two H bondings is different. The samples were also dried in a vacuum oven overnight at 60 °C, and their IR spectra were collected. In general, when the samples are dried, the loss of free water is seen, the carbonyl group related to ester does not change, and the carbonyl group related to amide (~1660 cm^{-1}) moves to a higher wavenumber for both the polymer and the polymer−clay composite.

Conclusion

In summary, the importance of the interfacial strength and the nanofiller structure in polymer−clay nanocomposites has been demonstrated using a designed polymer and nanocomposite synthesis. Interfacial interaction determines how the polymer chain interacts with the clay sheet, how an effective nanophase is formed, and how effective the new nanophase constrains the surrounding polymers. In our studied polymer−clay nanocomposites, the matrix chain mobility is largely decreased. The modulus enhancement strongly relates to the volume of the added clay as well as to the volume of the constrained polymer. It has been shown that the significant modulus enhancement of the polymer−clay nanocomposites follows a power law with the content of the clay and can be modeled well by Mooney's

equation. The modulus enhancement is dominated by the high aspect ratio of the clay platelet and the interfacial strength, through the Einstein coefficient, *K*, when the modulus of the matrix phase is much lower than that of the clay, i.e., $E_f/E_m > 100$. Our study also suggests that the structure of clay nanocomposites with strong interfacial interaction is analogous to that of semicrystalline polymers. In this clay nanocomposite, the intercalated clay phase serves as an unmeltable crystalline phase to result in the improvement of mechanical and thermal properties. Further work will focus on the quantitative measurement of the interfacial zone.

Acknowledgment. We thank David Decker for synthesizing the latex, Robert Kress and Nancy Furbeck for preparing the nanocomposite, Tonya Binga for DETA and DMTA measurement, and Thomas Blanton for X-ray diffraction measurement.

References and Notes

(1) Okada, A.; Usuki, A. *Mater. Sci. Eng., C* **1995**, *3*, 109.
(2) Usuki, A.; Kojima, M.; Okada, A.; Fukushima, Y.; Kurauchi, T.; Kamigaito, O. *J. Mater. Res.* **1993**, *8*, 1179.
(3) Usuki, A.; Kojima, M.; Kawasumi, M.; Okada, A.; Fukushima, Y.; Kurauchi, T.; Kamigaito, O. *J. Mater. Res.* **1993**, *8*, 1185.
(4) Maxfield, M.; Christiani, B. R. Patent PCT INt. Appl. WO 9311190, 1993.
(5) Southern Clay Products, datasheet.
(6) Sheng, N.; Boyce, M. C.; Parks, D. M.; Rutledge, G. C.; Abes, J. I.; Cohen, R. E. *Polymer* **2004**, *45*, 487.
(7) Vaia, R. A.; Sauer, B. B.; Tse, O. K.; Giannelis, E. P. *J. Polym. Sci., Part B: Polym. Phys.* **1997**, *35*, 59.
(8) Miltner, H. E.; Rahier, H.; Pozsgay, A.; Pukanszky, B.; Mele, B. V. *Compos. Interfaces* **2005**, *12*, 787.
(9) Shelley, J. S.; Mather, P. T.; DeVries, K. L. *Polymer* **2001**, *42*, 5849.
(10) Katti, K. S.; Sikdar, D.; Katti, D. R.; Ghosh, P.; Verma, D. *Polymer* **2006**, *47*, 403.
(11) Nagai, N.; Imai, T.; Fukasawa, R.; Kato, K.; Yamaushi, K. *Appl. Phys. Lett.* **2004**, *85*, 4010.
(12) Fornes, T. D.; Paul, D. R. *Polymer* **2003**, *44*, 4993.
(13) Rao, Y. *Polym. Compos.* **2006**, to be published.
(14) Wang, K. H.; Xu, M.; Choi, Y. S.; Chung, I. J. *Polym. Bull.* **2001**, *46*, 499.
(15) Sternstein, S. S.; Zhu, A. *Macromolecules* **2002**, *35*, 7262.
(16) Chisholm, B. J.; Moore, R. B.; Barber, G.; Khouri, F.; Hempstead, A.; Larsen, M.; Olson, E.; Kelley, J.; Balch, G.; Caraher, J. *Macromolecules* **2002**, *35*, 5508.
(17) Meheust, Y.; Sandnes, B.; Loevoll, G.; Maloey, K. J.; Fossum, J. O.; Da, Silva, G. J.; Mundim, M. S. P.; Droppa, R.; Fonseca, D. D. M. *Clay Sci.* **2006**, *12*, 66.
(18) Ogata, N.; Kawakage, S.; Ogihara, T. *J. Appl. Polym. Sci.* **1997**, *66*, 573.
(19) Alexander, L. E. *X-Ray Diffraction Methods in Polymer Science*; Wiley-Interscience: London, 1969.
(20) Negrete, Herrera, N.; Persoz, S.; Putaux, J.; David, L.; Bourgeat-Lami, E. *J. Nanosci. Nanotechnol.* **2006**, *6*, 421.
(21) Voorn, D. J.; Ming, W.; Van, Herk, A. M. *Macromolecules* **2006**, *39*, 2137.
(22) Daniel, V. *Dielectric Relaxation*; Academic Press: New York, 1967.
(23) Oka, S.; Chikahisa, Y. *Asalura Syoten* **1974**, *146*.
(24) Usuki, A.; Kojima, Y.; Kawasumi, M.; Okada, A. Y.; Kurauchi, T.; Kamigaito, O. *J. Appl. Polym. Sci.* **1995**, *55*, 119.
(25) Burnside, S. D.; Giannelis, E. P. *J. Polym. Sci., Part B: Polym. Phys.* **2000**, *38*, 1595.
(26) Wang, Z.; Pinnavaia, T. J. *Chem. Mater.* **1998**, *10*, 3769.
(27) Ward, I. M. *Mechanical Properties of Solid Polymers*; Wiley: London, 1971.
(28) Nielsen, L. E.; Landel, R. F. *Mechanical Properties of Polymer and Composites*; Marcel Dekker: New York, 1994.
(29) Nielsen, L. E. *J. Appl. Polm. Sci.* **1959**, *2*, 351.
(30) Mooney, M. *J. Colloid Sci*. **1951**, *6*, 162.

MA061445W